Journal of Medicinal Chemistry Article

J. Med. Chem. **2009,** *52,* 7273–7283 **7273**
DOI: 10.1021/jm901298x

A Novel Manganese Complex Effective as Superoxide Anion Scavenger and Therapeutic Agent against Cell and Tissue Oxidative Injury

Paola Failli,[†] Daniele Bani,[‡] Andrea Bencini,*[,§] Miriam Cantore,[†] Lorenzo Di Cesare Mannelli,[†] Carla Ghelardini,[†] Claudia Giorgi,[§] Massimo Innocenti,[§] Francesco Rugi,[§] Alessio Spepi,[§] Roberto Udisti,[§] and Barbara Valtancoli[§]

[†]*Department of Preclinical and Clinical Pharmacology and* [‡]*Department of Anatomy, Histology and Forensic Medicine, Section of Histology, University of Florence, V. le G. Pieraccini 6, Florence, Italy, and* [§]*Department of Chemistry, University of Florence, Via della Lastruccia 3, 50019 Sesto Fiorentino, Florence, Italy*

Received August 31, 2009

Two cyclic polyamine-polycarboxylate ligands, 1,4,7,10-tetraazacyclododecane-1,7-diacetic acid (H_2L3) and 4,10-dimethyl-1,4,7,10-tetraazacyclododecane-1,7-diacetic acid (H_2L4), and two noncyclic scaffolds, *N*-(2-hydroxyethyl)ethylenediamine-*N*,*N*′,*N*′-triacetic acid (H_3L1) and ethylene-bisglycol-tetracetic acid (H_4L2), form stable complexes with Mn(II) in aqueous solutions. Cyclic voltammograms show that the complexes with the most hydrophobic ligands, $[MnL2]^{2-}$ and [MnL4], are oxidized at higher potential than $[MnL1]^{-}$ and [MnL3]. The pharmacological properties of these molecules were evaluated as superoxide ion scavengers and anti-inflammatory compounds. Among the four complexes, [MnL4] was the most bioactive, being effective in the nanomolar/micromolar range. It abates the levels of key markers of oxidative injury on cultured cells and ameliorates the outcome parameters in animal models of acute and chronic inflammation. [MnL4] toxicity was very low on both cell cultures *in vitro* and mice *in vivo*. Hence, we propose [MnL4] as a novel stable oxygen radical scavenging molecule, active at low doses and with a low toxicity.

Introduction

Overproduction of harmful metabolic radicals overwhelming the endogenous catabolic systems is a major pathogenic mechanism of disease and aging. Although O_2 is required as the ultimate oxidant for cellular respiration, varying amounts of this molecule are reduced, through one-electron paths, to superoxide anion ($O_2^{\bullet -}$[a]). In a healthy organism, the endogenous levels of $O_2^{\bullet -}$ are limited by superoxide dismutases (SOD), contained in mitochondria (Mn-SOD), cytosol (Cu-/Zn-SOD), and outer plasma membrane (Cu-/Zn-SOD), which catalyze the dismutation of $O_2^{\bullet -}$ to O_2 and hydrogen peroxide by means of a transition metal at the active site.[1,2] In many chronic inflammatory and degenerative diseases, the production of $O_2^{\bullet -}$ is enhanced over the inactivating capability of SODs, thereby resulting in $O_2^{\bullet -}$-mediated cell injury.[3] Moreover, in animal models of inflammation and hyperalgesia induced by reactive oxygen species (ROS), Mn-SOD is rapidly inactivated,[4] thus allowing an increase in $O_2^{\bullet -}$ in inflamed tissues.

In this context, besides the classical anti-inflammatory drugs, extractive or recombinant Mn-SOD appeared to be the most logical choice for a causative therapeutic approach.[5] However, its actual clinical use has been hampered by multiple factors, including solution instability, limited cellular accessibility, immunogenicity, bell-shaped dose response curves, short half-life, and unfavorable yield/cost ratio.[6,7] Because of these limitations, pharmacological research pointed at nonpeptidic, low molecular weight SOD-mimicking compounds capable to catalyze $O_2^{\bullet -}$ dismutation with rates approaching that of the native Mn-SOD.[8] To this purpose, several manganese chelates with organic scaffolds have been synthesized and tested as anti-inflammatory drugs, including manganese complexes with phorphyrins,[9] salen,[10] and its derivatives and cyclic polyamines (Scheme 1).[11,12] Among these, Mn(II) chelates with macrocyclic pentaamines have shown good pharmacokinetic profile and specific $O_2^{\bullet -}$-scavenging properties in cellular and animal models.[13−15] Despite their promising features, these SOD-mimetics have not entered clinical use yet. Less attention has been paid to Mn(II) complexes with polyamine-polycarboxylate ligands. In principle, polyamine-polycarboxylate scaffolds may represent an optimal tool for the synthesis of stable Mn(II) complexes with anti-ROS properties. In fact, they are known for their ability to form highly stable metal chelates with many metal cations, from alkali and alkaline earth to transition and rare earth cations.[16] This property has been exploited in several industrial, biological, and medicinal applications.[17] Some of them are used, for instance, as additives of detergents to reduce the calcium hardness of water[18] and, in medicinal chemistry, as sequestering agents in the therapy of poisoning from heavy metals.[19] Some complexes with highly

*To whom correspondence should be addressed. Phone: +39-055-4573371, fax: +39-055-4573364, e-mail: andrea.bencini@unifi.it.

[a]Abbreviations: $O_2^{\bullet -}$, superoxide anion; SOD, superoxide dismutase; PBS, phosphate-buffered saline; NBT, Nitro blue tetrazolium; DMEM, Dulbecco′s modified essential medium; fMLP, *N*-formyl-Met-Leu-Phe peptide; RASM, Rat aorta smooth muscle cells; ICP-AES, inductively coupled plasma atomic emission spectrometer; MTT, 3-(4,5-dimethylthiozol-2-yl)-2,5-diphenyltetrazolium bromide; FBS, fetal bovine serum; TBARS, thiobarbituric acid reactive substances; i.p, intraperitoneal (administration); b.wt, body weight; p.o, oral administration (*per os*); S.E.M., standard errors of means; ANOVA, analysis of variance; cytC, cytochrome C ; ROS, reactive oxygen species.

Published on Web 10/27/2009

Scheme 1. Examples of Manganese Complexes with Phorphyrins (a, manganese(III)*meso*-tetrakis(*N*-ethylpyridinium-2-yl)porphyrin,) (AEOL 10113)),[9] Salen Derivatives (b, manganese(III)-[methoxy-*N*,*N*′-bis(salicyldene)ethylenediamine chloride][10] (EUK 134)), and Macrocyclic Polyamines (c, manganese(II)dichloro-{(4R,9R,14R,19R)-3,10,13,20,26-pentaazatetracyclo[20.3.1.0.^{4,9} 0^{14,19}]hexacosa-1(26),-22(23),24-triene} (M40403))[11,12] Used As SOD-Mimics

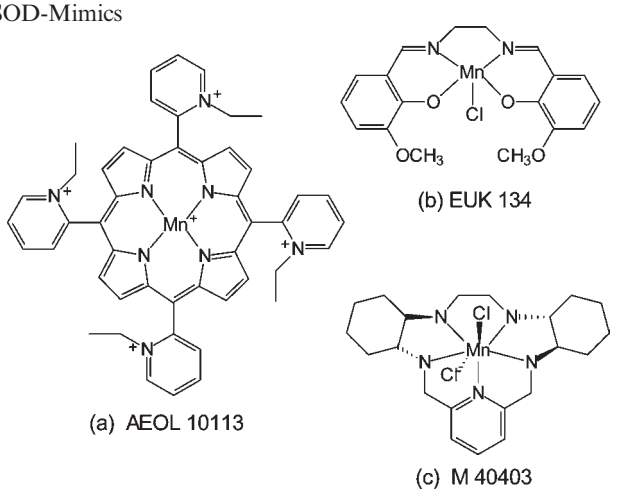

Scheme 2. Ligand Drawings

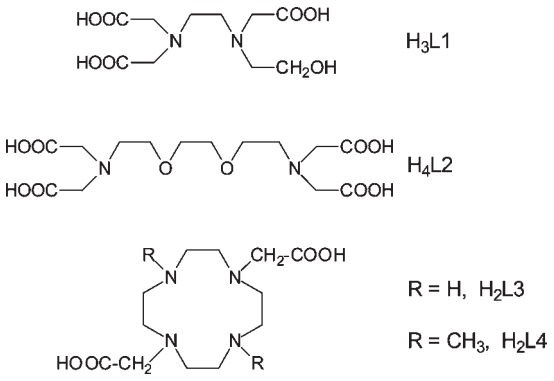

paramagnetic metal cations are currently employed in humans for diagnostic purposes, namely, the Gd(III) compounds used as contrast agents for nuclear magnetic resonance imaging.[20,21] In a pharmacological perspective, transition metal complexes with polyamine-polycarboxylic organic scaffolds have been shown to act as potent scavengers of nitrogen radicals.[22,23] Typically, these organic scaffolds have a low toxicity profile and are chemically stable, being resistant to oxidizing and reducing agents.[24] In comparison of Mn(II) complexes with previously reported polyamine ligands, the presence of the carboxylate groups may represent an important advantage, as they can bind to the metal and increase the thermodynamic stability of the complexes, thus reducing the possibility to release the metal in biological fluids. Furthermore, the negatively charged carboxylate units reduce the overall charge of the complex, which may favor a rapid and homogeneous biodistribution and facilitate the transfer across cell membranes.

On the above grounds, we designed the current study to investigate the chemical and biological activity as $O_2^{\bullet-}$-scavengers of some Mn(II) complexes with polyamine-polycarboxylate scaffolds. We used two open-chain ligands, *N*-(2-hydroxyethyl)ethylenediamine-*N*,*N*′,*N*′-triacetic acid (H_3L1) and ethylene-bisglycol-tetracetic acid (H_4L2) (Scheme 2) and two cyclic scaffolds, 1,4,7,10-tetraazacyclododenane-1,7-carboxylic acid (H_2L3) and 1,7-dimethyl-1,4,7,10-tetraazacyclododenane-4,10-carboxylic acid (H_2L4). In principle, Mn(II) binding gives rise to complexes with different coordination geometry, charge, hydrophobic characteristics, and redox properties, which may influence their $O_2^{\bullet-}$-scavenging ability. We have also tested the therapeutic efficacy of the complexes in animal models of inflammation. Comparison of the chemical and biological properties of the different compounds allowed us to identify the most suitable ones for pharmacological purposes, as well as to collect useful indications for drug design.

Table 1. Stability Constants and Thermodynamic Parameters for Mn(II) Complexation with H_3L1, H_4L2, H_2L3, and H_2L4 (I = 0.1 M, 25 °C)[a]

reaction	log *K*	$-\Delta H°$ (kJ mol^{-1})	$T\Delta S°$ (kJ mol^{-1})
		H_3L1	
$Mn^{2+} + L1^{3-} = [MnL1]^-$	11.96(1)[a]	15.8(8)	52.4(1)
		H_4L2	
$Mn^{2+} + L2^{4-} = [MnL2]^{2-}$	12.09 (2)	41.8(1)	27.2(1)
		H_2L3	
$Mn^{2+} + L3^{2-} = [MnL3]$	14.66(8)	23.6(1)	60.2(1)
$[MnL3] + H^+ = [Mn(HL3)]^+$	4.60(2)	32.9(1)	−6.8(1)
$[Mn(HL3)]^+ + H^+ = [Mn(H_2L3)]^{2+}$	4.01(1)	33.4(2)	−10.5(2)
		H_2L4	
$Mn^{2+} + L4^{2-} = [MnL4]$	14.73(2)	18.8(1)	64.9(1)
$[MnL4] + H^+ = [Mn(HL4)]^+$	4.53(7)	27.2(1)	−1.3(1)
$[Mn(HL4)]^+ + H^+ = [Mn(H_2L4)]^{2+}$	3.96(2)	26.1(1)	−3.3(1)

[a] Values are means ± SEM.

Results

Synthesis and Characterization of the Complexes. The complexes with H_2L3 and H_2L4 were prepared by mixing O_2-free solutions of ligands and metals at neutral pH under a nitrogen atmosphere, to avoid Mn(II) oxidation during the reaction of complex formation. The complexes were characterized by elemental analysis, which revealed the formation of complexes with 1:1 metal to ligand stoichiometry.

The formation of the Mn(II) complexes in aqueous solutions with ligands H_2L3 and H_2L4 was studied by potentiometric and microcalorimetric titrations in aqueous solutions (0.1 M NMe_4Cl, 25.0 °C). This method implies the preliminary determination of the thermodynamic parameters for protonation of the ligands. These values were in the range generally observed for polyaminocarboxylic acids[25] and are reported in the Supporting Information (Table S1). The formed species, their stability constants, and the enthalpic and entropic contributions to the processes of complex formation are shown in Table 1, while Figure 1 shows plots of the distribution curves of the complexes with H_2L3 and H_2L4 as a function of pH. The previously reported thermodynamic parameters for the complexes with H_3L1 and H_4L2[23] are also shown in Table 1 for comparison.

Analysis of the formed species revealed that Mn(II) gave stable 1:1 complexes in aqueous solutions with the fully deprotonated species of the four ligands tested. The complexes show a very weak tendency to bind acidic protons to give protonated species in aqueous milieu: indeed, only [MnL3] and [MnL4] produce very low concentrations of protonated complexes like $[Mn(H_xL3)]^{x+}$ and $[Mn(H_xL4)]^{x+}$ (x = 1 or 2). As often observed for metal complexes with polyamine-polycarboxylate scaffolds, in the $[MnL1]^-$, $[MnL2]^{2-}$, [MnL3], and [MnL4] the carboxylate

groups are likely bound to the metal, as sketched in Scheme 3 for the [MnL3] and [MnL4] complexes. This makes the process of proton binding unlikely and unfavored, as this would imply detachment of the coordinated carboxylate group from the metal center. The Mn(II) complexes with all ligands are completely formed in aqueous solutions above pH 5−6, and no free metal was present in solution at neutral pH (see Figure 1 for H_2L3 and H_2L4 and Supporting Information, Figure S1, for H_3L1 and H_4L2).

Table 1 also shows that both enthalpy and entropic changes promote the formation of the complexes. However, with the only exception of $[MnL2]^{2-}$, the entropic terms are largely predominant, as expected considering that entropically driven reactions are typical of complexation processes in which charge neutralization plays a major role. When comparing stability of the Mn(II) metal complexes (Table 1), [MnL3] and [MnL4], i.e., the complexes with the two cyclic scaffolds, were remarkably more stable than those formed by the two open-chain ligands, $[MnL1]^-$ and $[MnL2]^{2-}$. The higher stability of the Mn(II) complexes with H_2L3 and H_2L4 is conceivably related to the larger entropic contribution to their formation.

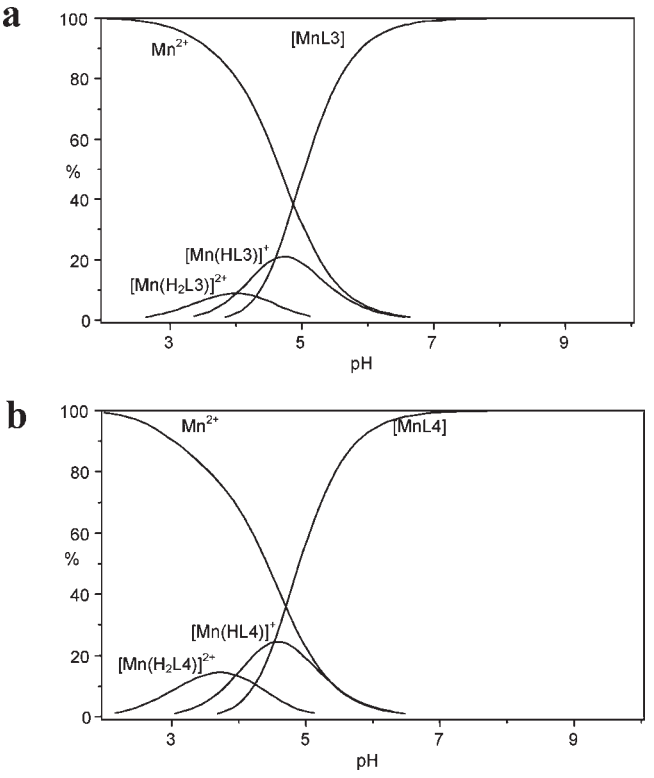

Figure 1. Distribution curves of the complexes with H_2L3 (a) and H_2L4 (b) (25 °C, I = 0.1 M).

Scheme 3. Proposed Binding Mode of $L3^{2-}$ and $L4^{2-}$ in the [MnL3] and [MnL4] Complexes

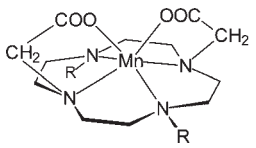

R = H, [MnL3]

R = CH_3, [MnL4]

The cellular and extracellular environments contain a large amount of metal cations, such as K(I), Na(I), Ca(II), and Mg(II), which could form stable complexes with polyamine-polycaboxylate ligands. For this reason, we determined the stability of the noted compounds in the presence of the above metal cations by potentiometric titrations (Table 2). The stability of the K(I) complexes is too low to be confidently determined (log K < 2). Although the stability constants of complexes with H_3L1 and H_4L2 are already known,[26,27] they have been redetermined in the current experimental conditions to achieve comparable sets of data. Table 2 shows that Na(I), Ca(II), and Mg(II) formed markedly less stable complexes than Mn(II) with all four ligands. To assess whether Na(I), Ca(II), and Mg(II) could compete with Mn(II) in the complexation process, we considered competitive systems containing each ligand and Mn(II) at very low concentrations (1 μM) in the presence of excess Na(I) (165 mM), Ca(II) (2.5 mM) and Mg(II) (1.2 mM). This solution composition roughly reproduces that of the medium used in the biological experiments. We then calculated the overall percentages of the different metal cations complexed with each ligand over a wide pH range.[28,29] As shown in the competition diagrams reported in Figure 2 (for H_3L1 and H_2L4) and in Figure S2 of the Supporting Information (for H_3L2 and H_2L3), Ca(II) competes with Mn(II) for complexation to H_3L1 and H_4L2. In fact, Mn(II) is partially released from H_3L1 or completely from H_4L2 upon Ca(II) and/or Mg(II) complexation (see Figure 2a and Supporting Information, Figure S1). Conversely, Mn(II) remains completely complexed to H_2L3 and H_2L4, as Ca(II), Mg(II), and Na(I) were basically not bound by these ligands (Figure 2b and Supporting Information Figure S2). Of note, Mn(II) release from [MnL3] and [ML4] does not take place even using higher Ca(II), Mg(II), or Na(I) concentrations ([Ca(II)] = [Mg(II)] = 10 mM, [Na(I)] = 200 nM) (see Supporting Information, Figure S3).

Electrochemical Properties of the Complexes. The redox properties of the complexes were analyzed by cyclic voltammetry. Figure 3 reports the cyclic voltammograms for oxidation of the four manganese complexes. $[MnL1]^-$, $[MnL2]^{2-}$, and [MnL3] show successive broad, partially overlapped oxidation peaks, while [MnL4] shows a single sharp peak at about 1.15 V. The onset potentials, e.g., the potentials where the complexes start oxidizing were 0.80, 0.46, 0.49, and 0.86 for $[MnL1]^-$, $[MnL2]^{2-}$, [MnL3], and [MnL4], respectively; and all the observed redox processes were irreversible. The single oxidation process displayed by [MnL4] was also studied by recording voltammograms (Figure 4a) with different scan rates (in the case of the other complexes, this

Table 2. Stability Constants of the Na(I), Mg(II), and Ca(II) Complexes with H_3L1, H_4L2, H_2L3, and H_2L4 (I = 0.1 M, 25 °C)

					log K	
reaction	log K	reaction	log K	reaction	L = L3	L = L4
$Na^+ + L1^{3-} = [NaL1]^{2-}$	2.60(9)	$Na^+ + L2^{4-} = [NaL2]^{3-}$	2.72(7)	$Na^+ + L^{2-} = [NaL]^-$	2.17(5)	2.08(7)
$Ca^{2+} + L1^{3-} = [CaL1]^-$	7.59(7)	$Ca^{2+} + L2^{4-} = [CaL2]^{2-}$	11.75(8)	$Ca^{2+} + L^{2-} = [CaL]$	8.05(1)	7.67(8)
		$[CaL2]^{2-} + H^+ = [CaHL2]^-$	3.62(3)			
$Mg^{2+} + L1^{3-} = [MgL1]^-$	6.23(5)	$Mg^{2+} + L2^{4-} = [MgL2]^{2-}$	5.64(7)	$Mg^{2+} + L^{2-} = [MgL]$	5.91(6)	5.74(7)

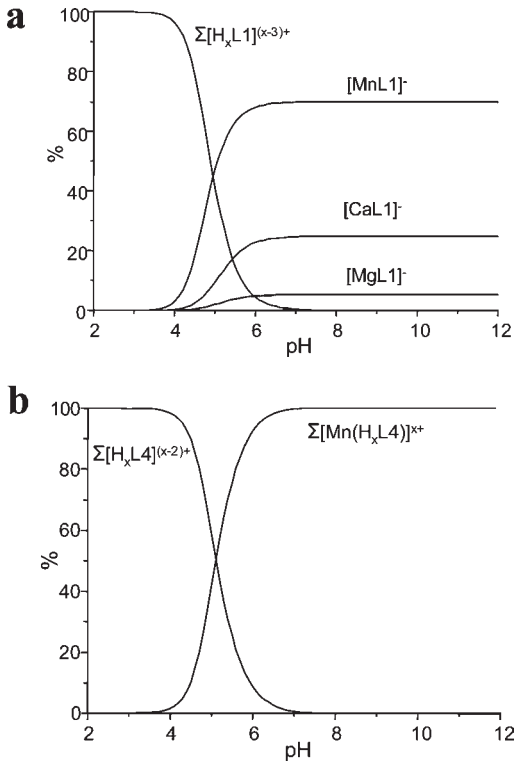

Figure 2. Overall percentages of the H_3L1 (a) and H_2L4 (b) complexed species with Mn(II), Ca(II), Mg(II), and Na(I) as a function of pH in competitive systems containing Mn(II) (1 μM), Ca(II), (2.5 mM), Mg(II) (1.5 mM), and Na(I) (165 mM) and H_3L1 (1 μM) or H_2L4 (1 μM). $\sum[Mn(H_xL4)]^{x+} = [MnL4] + [Mn(HL4)]^{+} + [Mn(H_2L4)]^{2+}$; $[\sum[H_xL1]^{(x-3)+} = [L1]^{3-} + [HL1]^{2-} + [H_2L1]^{-} + [H_3L1]$; $[\sum[H_xL4]^{(x-2)+} = [L4]^{2-} + [HL4]^{-} + [H_2L4] + [H_3L4]^{+} + [H_4L4]^{2+}$.

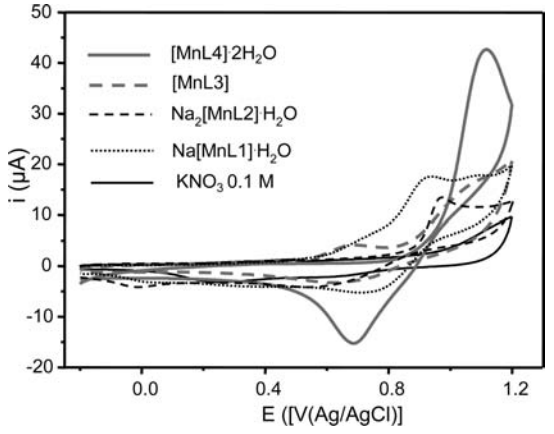

Figure 3. Cyclic voltammograms for oxidation of $[MnL4]\cdot 2H_2O$, [MnL3], $Na_2[MnL2]\cdot H_2O$, and $Na[MnL1]\cdot H_2O$, on gold electrode in KNO_3 0.1 M solution with a sweep rate of 50 mV/s ([complex] = 5×10^{-4} M, pH 7, and T = 25 °C). The cyclic voltammogram of 0.1 M pure KNO_3 in the same conditions is also shown.

analysis was prevented by the wide shape of the peaks and/or by their extensive overlapping). In fact, analysis of the potential of the oxidation peaks (E_p) at different scan rates can give information on the nature of the step that controls the rate of the oxidation process as well as on the number of electrons involved in this process. In fact, for an irreversible anodic process, E_p is related to the scan rate (v_s) by eq 1:[30]

$$E_p = K - (2.3RT/2\alpha_a F) \log v_s \quad (1)$$

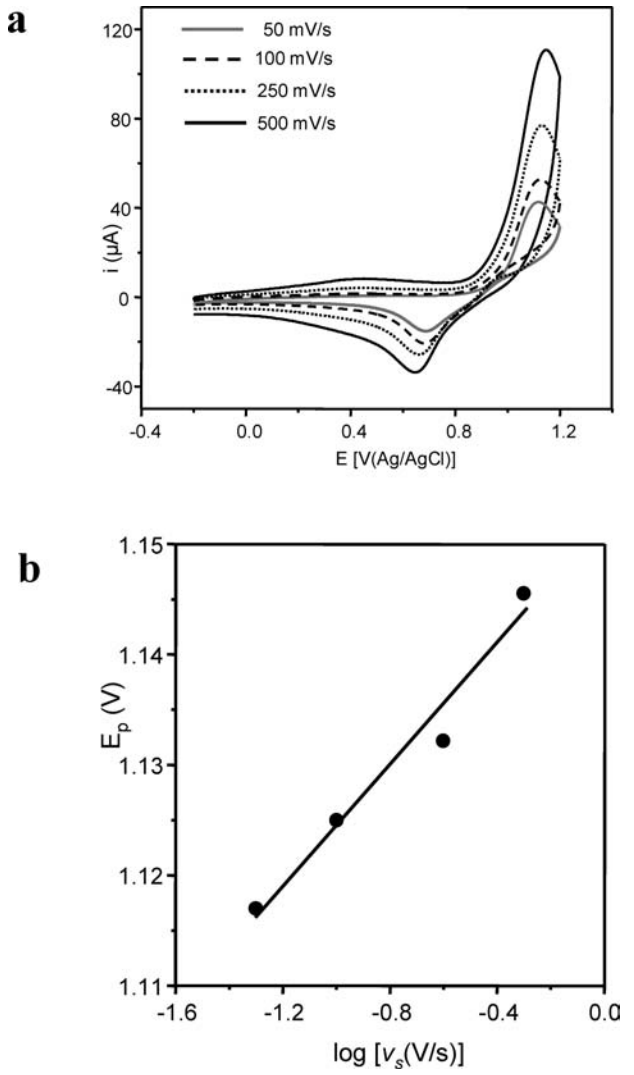

Figure 4. Cyclic voltammagrams of the $[MnL4]\cdot 2H_2O$ complex at different scan rates (pH 7, 25 °C, I = 0.1 M) (a) and plot of the potential of the oxidation peaks vs scan rate (b).

where K is a constant and α_a depends on the number of electrons, n_a, involved in the steps preceding the rate determining step (r.d.s) and on the charge transfer coefficient β, as expressed by eq 2:

$$\alpha_a = n_a + r(1 - \beta) \quad (2)$$

Here, r is a parameter that can assume two different values; that is, r = 0 in the case of a chemical r.d.s or r = 0.5 in the case of an electrochemical r.d.s.

In the present case, an α_a value of 1.07 could be determined by the slope of the line obtained by plotting E_p values at different scan rates (Figure 4b). According to eq 2, this value can be rationalized considering a monoelectronic oxidation process (n_a = 1), whose rate is chemically controlled (r = 0).

Scavenging of $O_2^{\bullet -}$ Generated by Xanthine/Xanthine Oxidase. The scavenging properties of the Mn(II) complexes were first evaluated by analyzing the time-course of NBT oxidation induced by the xanthine/xanthine oxidase as source of $O_2^{\bullet -}$ (Table 3). In control conditions, the NBT oxidation was complete in 498 ± 35.6 s, 50% of maximal NBT oxidation being achieved after about 290. The xanthine oxidase inhibitor allopurinol (100 μM) strongly modified the kinetic of NBT oxidation by shifting the time-course curve to

Table 3. Effect of the Polyamine-Polycarboxylate Mn(II) Complexes (10 μM) on the Time (s) Needed to Attain 50% Maximal NBT Oxidation upon Exposure to $O_2^{\bullet-}$ Generated by Xanthine/Xanthine Oxidase

control	Na[MnL1]	Na_2[MnL2]·H_2O	[MnL3]	[MnL4]·$2H_2O$	H_2L4
294 ± 12.3^a	420 ± 41.5^b	364 ± 14.0	306 ± 27.2	390 ± 15.9^b	332 ± 24.6

[a] Values are means ± SEM. Each group, $n = 4$. [b] $p < 0.05$ vs controls (one-way ANOVA and Bonferroni's posthoc test).

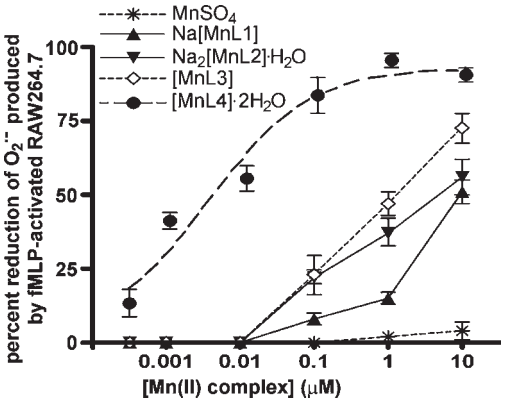

Figure 5. Effect of polyamine-polycarboxylate Mn(II) complexes and $MnSO_4$ on the levels of superoxide anion ($O_2^{\bullet-}$) produced by RAW264.7 stimulated with 0.1 μM fMLP. Data are expressed as percent reduction of $O_2^{\bullet-}$ produced by fMLP-challenged RAW264.7. The basal $O_2^{\bullet-}$ production was 1.3 ± 0.96 mmol/mL/4 h (10^6 cells) and 4.2 ± 0.78* mmol/mL/4 h (10^6 cells) after 0.1 μM fMLP ($n = 4$, $^*p < 0.05$).

the right in nonparallel mode. The time-course curve of NBT oxidation was shifted to the right in a parallel mode by 10 μM Na[MnL1] and [MnL4]·$2H_2O$. Both these compounds significantly increased the time required to oxidate 50% of NBT (Table 3), leaving maximum NBT oxidation unchanged. In parallel experiments, the production of uric acid by xanthine/xanthine oxidase was not modified by Na[MnL1] and [MnL4]·$2H_2O$ (10 μM), suggesting that their inhibitory effect on NBT oxidation was not dependent on the blockade of xantine oxidase enzymatic activity, as did allopurinol, but rather on specific quenching of $O_2^{\bullet-}$. [MnL2]·H_2O and [MnL3] were almost ineffective.

Scavenging of $O_2^{\bullet-}$ Generated by Activated Macrophages. The scavenging properties of the Mn(II) complexes were further evaluated on $O_2^{\bullet-}$ produced by activated RAW264.7 cells (Figure 5). Compared with unstimulated cells, addition of fMLP (0.1 μM) caused a 3-fold, statistically significant elevation of $O_2^{\bullet-}$ production (from 1.32 ± 0.19 to 4.2 ± 0.78 μmol/mL/10^6 cells, $P < 0.05$, $n = 4$). All the Mn(II) complexes reduced the levels of $O_2^{\bullet-}$ released by fMLP-stimulated RAW264.7 cells, whereas $MnSO_4$ was ineffective. Among these compounds, [MnL4]·$2H_2O$ was the most potent in preventing $O_2^{\bullet-}$-dependent cytC oxidation. Indeed, it was capable of reducing cytC oxidation in a concentration-related fashion in the 1 nM to 1 μM range, with its IC_{50}% being 59.2 ± 6.13 nM. By comparison, the other compounds were less effective, with their concentration−response curves in the 0.1−10 μM range.

Intracellular Distribution of the Mn(II) Complexes. The higher effectiveness of [MnL4]·$2H_2O$ in comparison to the other Mn(II) compounds could be related to its higher lipophilic properties, that can favor its trans-membrane passage and distribution in the intracellular compartment. To test this hypothesis, RASM cells were incubated for 6 h

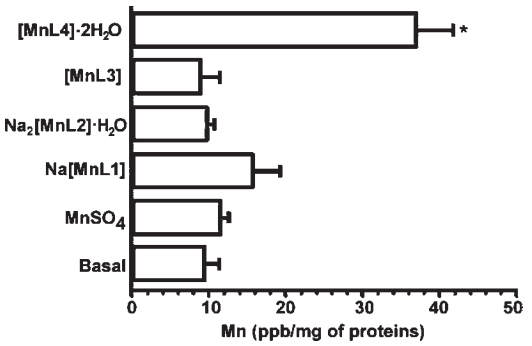

Figure 6. Total content of manganese in homogenates of RASM cells incubated in the absence (basal) or the presence of the Mn(II) complexes (1 μM) or $MnSO_4$ (1 μM) for 6 h. Values are reported as means ± SEM. Significance of differences (one-way ANOVA, $n = 3$): $^*p < 0.05$ vs the other groups.

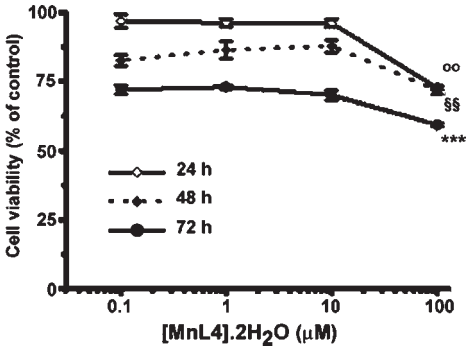

Figure 7. Viability of RAW264.7 cells, evaluated with the MTT assay, upon 24, 48, and 72 h incubation of the cultures with [MnL4]·$2H_2O$. Values are expressed as percentage of the untreated controls. Significance of differences (one-way ANOVA followed by Bonferroni's t test): $^{***}p < 0.001$ 72 h vs control, 24 and 48 h curves (all doses); §§ $p < 0.01$, 48 h vs. control and 24 h (all doses); °° $p < 0.01$ 24 h vs control (100 μM).

with the different Mn(II) compounds (1 μM) or $MnSO_4$ (1 μM) for 6 h and the total intracellular manganese content, determined by ICP-AES measurements, is shown in Figure 6. In control cultures, basal manganese cell content was 8.6 ± 2.89 ppb/mg of proteins ($n = 3$). Preincubation with [MnL4]·$2H_2O$ increased significantly intracellular manganese content, whereas preincubation with the other Mn(II) compounds did not yield any significant increase over the basal manganese levels. On the basis of these data, [MnL4]·$2H_2O$ was selected for further investigations. Assuming that this compound can cross the plasma membrane, RAW267.4 cells were preincubated with culture medium containing 10 μM [MnL4]·$2H_2O$ for 18 h, which was then replaced with plain medium before fMLP stimulation. Even in these conditions, [MnL4]·$2H_2O$ prevented by 72% $O_2^{\bullet-}$-dependent cytC oxidation, as occurred when the compound was present in the culture medium during fMLP stimulation (98.9% inhibition).

***In Vitro* and *in Vivo* Toxicity of [MnL4]·$2H_2O$.** We next investigated [MnL4]·$2H_2O$ toxicity on RAW264.7 cells. Cell viability was assessed after 24, 48, and 72 h incubation in culture medium added with this compound in the 0.1−100 μM range (Figure 7). At 24 h, [MnL4]·$2H_2O$ only reduced cell viability by 27% at the higher concentration tested (100 μM), which is 100-fold higher than that capable to fully abate $O_2^{\bullet-}$ levels in fMLP-activated RAW264.7 cell cultures. At 48 and 72 h, cell viability was reduced in a

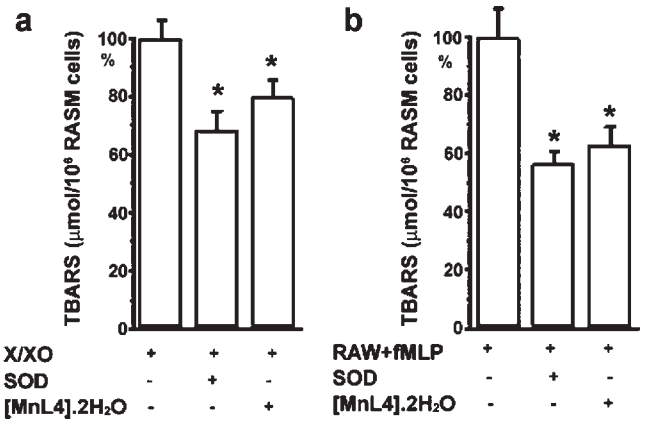

Figure 8. Effect of MnSOD (300 U/mL) and $[MnL4]\cdot 2H_2O$ (10^{-7} M) on inhibition of lipid peroxidation, measured as TBARS amounts, induced in RASM cells by $O_2^{\bullet -}$, generated by (**a**) xanthine/xanthine oxidase (X/XO) or (**b**) fMLP-stimulated RAW264.7 cells. Values are mean ± SEM of at least 4 experiments and are expressed as a percentage of the positive controls. Significance of differences (one-way ANOVA followed by Bonferroni's *t* test): $*p < 0.05$ vs the positive controls (left bar).

concentration-dependent fashion; however, at the highest 100 μM concentration, it remained at 72% and 60% of the time-matched untreated cultures, respectively.

To evaluate the *in vivo* toxicity of $[MnL4]\cdot 2H_2O$, this compound was administered i.p. to male albino CD1 mice at the doses of 200 and 400 mg/kg b.wt (each group, $n = 5$), which are 20−40-fold higher than those found to have therapeutic properties. At these doses, no signs of acute toxicity were observed within the first 4 h after administration, nor did any animal die in the following 7 days.

Scavenging of $O_2^{\bullet -}$ Prevents Oxidative Cell Injury. Excess ROS have been shown to target cell membrane lipids, causing an increase in thiobarbituric acid reactive substances (TBARS) which are considered a reliable index of oxidative cell/tissue injury.[31] Therefore, we evaluated the scavenging properties of $[MnL4]\cdot 2H_2O$ on RASM cells in which lipid peroxidation was induced by $O_2^{\bullet -}$ generated by either xantine/xantine oxidase or fMLP-activated RAW264.7 cells. As shown in Figure 8a, addition of xanthine/xanthine oxidase to the culture medium of RASM cells for 4 h significantly increased TBARS of about 3-fold over the basal levels. Addition of $[MnL4]\cdot 2H_2O$ (0.1 μM) reduced the TBARS levels by about 21%. By comparison, addition of Mn-SOD (300 U/mL) reduced the TBARS levels by about 32%. Since in parallel experiments monitoring uric acid production by xanthine/xanthine oxidase we observed that $[MnL4]\cdot 2H_2O$ had no enzyme inhibitory effects, we can argue that the antioxidant action of $[MnL4]\cdot 2H_2O$ does depend on effective $O_2^{\bullet -}$ quenching.

Similar results were obtained when $O_2^{\bullet -}$ was generated by fMLP-activated RAW264.7 cells coincubated with RASM cells (Figure 8b). TBARS levels in RASM cells cultured alone or in the presence of quiescent RAW264.7 macrophages were very low. Upon stimulation of RAW264.7 cells with 0.1 μM fMLP, TBARS levels increased significantly. On the other hand, preincubation with either $[MnL4]\cdot 2H_2O$ (0.1 μM) or MnSOD (300 U/mL) reduced fMLP-induced TBARS elevation by 37% and 45%, respectively. Of note, neither $[MnL4]\cdot 2H_2O$ nor MnSOD reduced TBARS elevation induced in RASM cells by the addition of Fe(III)/ascorbic acid, an experimental system able to generate hydroxyl radical. This finding accounts for the specificity of $[MnL4]\cdot 2H_2O$ as a selective $O_2^{\bullet -}$ scavenger.

Table 4. Effects of $[MnL4]\cdot 2H_2O$, the Metal-Free Congener H_2L4 and Indomethacin in the Mouse Writhing Test

	no. of mice	time before acetic acid	dose (mg/kg b.wt)	no. of writhes[a]
		p.os Treatment		
controls (1% CMC)	19	15 min	-	41.8 ± 1.5
Indomethacin	5	15 min	10	18.0 ± 1.8*
$[MnL4]\cdot 2H_2O$	6	15 min	1	40.0 ± 1.8
$[MnL4]\cdot 2H_2O$	8	15 min	5	28.3 ± 1.6**
$[MnL4]\cdot 2H_2O$	8	15 min	15	27.8 ± 1.3**
$[MnL4]\cdot 2H_2O$	6	30 min	15	33.3 ± 1.3*
H_2L4	7	15 min	5	30.3 ± 2.0*
H_2L4	8	15 min	15	34.2 ± 2.1*
i.p. treatment				
Controls (saline)	8	15 min	-	38.5 ± 1.6
$[MnL4]\cdot 2H_2O$	8	15 min	1	36.7 ± 2.2
$[MnL4]\cdot 2H_2O$	8	15 min	5	24.3 ± 1.7**
$[MnL4]\cdot 2H_2O$	8	15 min	15	21.9 ± 1.9**
H_2L4	9	15 min	5	39.6 ± 2.0
H_2L4	9	15 min	15	37.8 ± 2.5

[a] Values are means ± SEM. $*p < 0.05$; $**p < 0.01$ versus CMC-treated mice (one way ANOVA and Bonferroni's posthoc test).

Anti-Inflammatory Activity of $[MnL4]\cdot 2H_2O$ *in Vivo*. As shown in Table 4, a 15 min pretreatment with $[MnL4]\cdot 2H_2O$ at the doses of 5 and 15 mg/kg b.wt significantly and dose-dependently reduced the number of writhes caused by acetic acid-induced acute peritoneal inflammation, regardless of the administration route (p.os: 67.7% and 66.5% of the positive controls, respectively; i.p.: 63% and 56.9% of the positive controls, respectively). At these doses, this compound did not cause any reduction of consciousness or spontaneous motility of the treated mice. By comparison, p.os or i.p. treatment with indomethacin (10 mg/kg b.wt) reduced the numbers of whites to 43% and 46.7% of the positive controls, respectively. On the other hand, H_2L4, the organic scaffold lacking functional Mn(II) ion, showed a modest anti-nociceptive activity when administered p.os (81.8% of the positive controls with 15 mg/kg b.wt) but was ineffective when administered i.p. at any dose. This is conceivably due to its free amine and carboxylic functions, which could avidly bind endogenous Mn(II), thereby transforming this compound into an active $O_2^{\bullet -}$ quencher. In this case, H_2L4 may behave as a pro-drug.

Tested at the same doses by i.p. route, $[MnL4]\cdot 2H_2O$ was ineffective in the hot plate test, thus suggesting that the molecule possesses anti-inflammatory properties, but not pure analgesic morphine-like activity.

Discussion and Conclusions

The present study offers evidence that Mn(II) complexes with polyamine-polycarboxylate scaffolds may be effective $O_2^{\bullet -}$ scavengers in biological systems and, therefore, may prevent oxidative cell/tissue damage and exert anti-inflammatory therapeutic effects. In aqueous solutions at physiological pH, temperature, and molarity, Mn(II) formed stable complexes with all the tested ligands in their fully deprotonated forms, and no detectable metal release was observed. The high stability of the complexes is justified by the simultaneous involvement in metal binding of both the amine donor atoms and the negatively charged carboxylate groups, as shown in Scheme 3 for [MnL3] and [MnL4].

Of note, the complexes of Mn(II) with the cyclic ligands H_2L3 and H_2L4 show a higher stability than those with H_3L1 and H_4L2. This result can be explained by the presence of a higher number of amine groups available for metal coordination as compared with the open-chain scaffolds, as well as by their cyclic structure. In fact, macrocyclic ligands are known to form more stable complexes than their noncyclic counterparts.[16] From a thermodynamic point of view, the higher stability constants found for [MnL3] and [MnL4] are related to the larger entropic contribution to metal complexation, which can be reasonably due to a larger desolvation of the metal ion upon complexation, in keeping with the proposed structure reported in Scheme 3, which shows that the metal center is coordinatively saturated by the four amine donors and the two carboxylate groups.[32] Furthermore, the cyclic structure of H_2L3 and H_2L4 make them more rigid than H_2L2 and H_2L1. The consequent lower loss of conformational freedom upon Mn(II) coordination can lead to a further entropic stabilization of the [MnL3] and [MnL4] complexes with respect to the $[MnL1]^-$ and $[MnL2]^{2-}$ ones.

The addition of carboxylate groups to the structure of simple cyclic or acyclic polyamines may represent an added value to the Mn(II) complexes in view of their use as $O_2^{\bullet-}$-scavengers. In fact, binding of carboxylate groups to Mn(II) markedly increases stability of the complex, thus avoiding metal release in solution. For instance, the stability constants of the [MnL3] and [MnL4] complexes are more than 4 orders of magnitude higher than the Mn(II) complexes with macrocyclic polyamines containing 4, 5, or 6 secondary nitrogen donors.[33] Furthermore, the presence of the anionic carboxylate groups lead to the formation of neutral complexes, at least in the case of [MnL3] and [MnL4], making them more suitable for transfer processes across lipophilic membranes. From this point of view, the presence of two N-Me groups within the backbone of H_2L4 makes [MnL4] less solvatated and more lipophilic than [ML3].

Although all four ligands tested can also bind Mg(II), Ca(II), and Na(I), the [MnL3] and [MnL4] complexes do not release Mn(II) at physiological pH even in the presence of a large excess of these potentially competitive metal cations. In fact, in a simulated environment roughly reproducing the metal ion composition of biological fluids, only $[MnL2]^{2-}$ and, to a lesser extent, $[MnL1]^-$, released Mn(II) due to Ca(II) and Mg(II) complexation, while the other Mn(II) complexes were not affected by the metal ion competitors in the medium. This finding can address the major safety concerns about the *in vivo* use of the complexes of Mn(II) with the cyclic ligands H_2L3 and H_2L4, as it shows that no metal ion release may occur in physiological extracellular or intracellular milieu.

Since the process of $O_2^{\bullet-}$ scavenging is related to oxidation processes involving the metal center, we then analyzed the redox properties of the complexes by cyclic voltammetry. The complexes displayed a markedly different tendency to oxidation, $[MnL2]^{2-}$ and [MnL4] being oxidized at remarkably higher potential than $[MnL1]^-$ and [MnL3]. This result can be explained in terms of scarcely solvated hydrophobic environments surrounding the metal cations, which normally stabilize the lower oxidation states.[34] In fact, the presence of a hydrophobic polyether chain in H_4L2 or of two methylated nitrogen donors in H_2L4, which prevent the formation of $H_2O\cdots HN$ hydrogen bonds, can reduce the overall solvation of their complexes, making them more resistant to oxidation. In the case of the $[MnL1]^-$, $[MnL2]^{2-}$, and [MnL3] the first oxidation step, which is probably due to a Mn(II) → Mn(III) process, was followed by other partially overlapped oxidation steps at the metal centers, which cannot be clearly identified. Conversely, [MnL4], the most oxidation-resistant complex, only displayed a monoelectronic single oxidation step, suitable for more detailed electrochemical characterization. In particular, the fast electron transfer step was followed by a slow chemical process, which represents the rate-determining step (r.d.s) of the overall $[Mn(II)L] \rightarrow [Mn(III)L]^+$ process. This r.d.s can be reasonably identified with a rearrangement of the set of donors of the ligand around the generated Mn(III) ion, in keeping with the general consideration that rearrangement processes of the metal coordination spheres are remarkably slower than electron transfer processes.[30] At the same time, an overall rearrangement of the ligand structure around the Mn(III) cation is conceivable on the basis of its different positive charge and electronic configuration with respect to Mn(II).

In turn, the biological findings demonstrate that $[MnL4]\cdot 2H_2O$ is a potent scavenger of $O_2^{\bullet-}$ radicals generated by both exogenous and endogenous pathways, being able to exert statistically significant effects in the low micromolar−high nanomolar range. Among the studied Mn(II) complexes, $[MnL4]\cdot 2H_2O$ has emerged as the most promising $O_2^{\bullet-}$ scavenger because of its superior chemical stability. In fact, only [MnL4] did show clear-cut $O_2^{\bullet-}$ scavenging properties in the *in vitro* cell models, allowing us to select this for the *in vivo* assays. The higher efficacy of $[MnL4]\cdot 2H_2O$ compared to the other Mn(II) compounds tested may conceivably depend on several distinctive chemical properties of this molecule. First, the $[MnL4]\cdot 2H_2O$ complex is partially lipophilic and not charged and can effectively cross the cell membranes, thereby scavenging $O_2^{\bullet-}$ directly into the cell, where ROS are generated, and blunting the oxidative cascade *ab initio*. Second, according to the data of cyclic voltammetry, $[MnL4]\cdot 2H_2O$ is highly resistant to oxidation, thus maintaining its chemical integrity and $O_2^{\bullet-}$-scavenging properties for a long time even in the presence of harmful, inflammation-induced oxidative burst. Third, $[MnL4]\cdot 2H_2O$ is highly stable and does not release Mn(II), accounting for its low toxicity both *in vivo* and *in vitro*.

Of note, $[MnL4]\cdot 2H_2O$ protects cell lipid peroxidation when oxidation is induced by $O_2^{\bullet-}$, but not when hydroxyl radicals play a predominant role. This implies a specific mechanism of action for $[MnL4]\cdot 2H_2O$ which selectively targets $O_2^{\bullet-}$. In keeping with this finding, MnSOD is also unable to reduce lipid peroxidation by a hydroxyl radical, indicating that the Mn(II) core is crucial for $O_2^{\bullet-}$ dismutation and suggesting that $[MnL4]\cdot 2H_2O$ can function as a SOD-mimetic drug.

A large body of evidence indicates that $O_2^{\bullet-}$ radical plays a key role in the pathogenesis of several inflammatory and degenerative diseases. Moreover, in these pathological conditions, endogenous SOD is rapidly oxidized and inactivated, thus leading to ever-increasing concentrations of this harmful radical.[3,4] On these grounds, we have tested the therapeutic efficacy of $[MnL4]\cdot 2H_2O$ in a model of inflammatory pain in the mouse, and we observed that this molecule exerts clear-cut anti-inflammatory effects when administered p.os and i.p. This finding further suggests that the lipophilic features of this molecule allow its easy absorption and distribution within the body. On the contrary, $[MnL4]\cdot 2H_2O$ is ineffective in the relief of noninflammatory pain as determined on hot plate test. This is in line with our hypothesis that $[MnL4]\cdot 2H_2O$

primarily acts as an $O_2^{\bullet-}$ scavenger and does not interfere with other inflammation-triggered metabolic pathways. In particular, $[MnL4]\cdot 2H_2O$ does not reduce prostaglandin production, as tested by EIA (not shown), indicating that the molecule does not act as a traditional nonsteroidal anti-inflammatory drug.

In conclusion, our data show that several polyamine-polycarboxylic-manganese compounds can function as $O_2^{\bullet-}$ scavengers in biological systems. Among the tested compounds, the lipophilic complex $[MnL4]\cdot 2H_2O$ has emerged as a novel, chemically stable, potent $O_2^{\bullet-}$ scavenger with safe toxicity profile and optimal pharmacokinetic properties, allowing it to attain therapeutic levels in the extracellular and intracellular compartments. As such, $[MnL4]\cdot 2H_2O$ represents a promising member of a new class of MnSOD-mimetic anti-inflammatory drugs.

Experimental Section

Chemicals. Unless otherwise specified, the general purpose chemicals used in this study were from Sigma-Aldrich (Milan, Italy). All tissue culture media, supplements, growth factors, and phosphate-buffered saline (PBS) were from Gibco/BRL (Invitrogen, S.Giuliano Milanese, Italy). Cell culture disposable plasticware was from Falcon (Steroglass, Perugia, Italy) or Corning (VWR International, Milan, Italy). The aqueous solutions used in complex synthesis, in potentiometric and calorimetric measurements, were deoxygenated by bubbling N_2 to prevent possible oxidation of Mn(II). H_3L1 and H_4L2 were purchased from Aldrich (purity ≥99%). ^1H and ^{13}C spectra were recorded on a Varian Gemini 300 MHz Instrument. ESI-MS spectra were recorded on a LTQ Orbitrap high-resolution mass spectrometer, equipped with a conventional ESI source. Elemental analyses (C, H, N content) were performed with Perkin-Elmer 2400 CHN elemental analyzer. The determination of the manganese content of the complexes was performed using a Varian 720-ES inductively coupled plasma atomic emission spectrometer (ICP-AES). For all tested compounds, satisfactory elemental analyses were obtained (all determined C, H, N, and Mn percentages are within ±0.2% of theoretical value, with the only exception of the Mn percentage in [MnL4] (+0.25%); see Table S1, Supporting Information), in keeping with a >95% purity for all compounds.

Synthesis of H_2L4 and Mn(II) Complexes. H_2L3,[35] Na-[MnL1], and $Na_2[MnL2]\cdot H_2O$ were prepared as previously described.[23] H_2L4 was synthesized according to a Vizza et al.,[36] with minor modifications.

Synthesis of $H_2L4\cdot 3HCl$. A solution of chloroacetic acid (5.98 g, 63 mmol) in water (10 mL) was added to a solution of 1,7-dimethyl-1,4,7,10-tetraazacyclododecane (1.26 g, 6.3 mmol) in water (10 mL), adjusting pH to 9.5 by using a 5 M NaOH solution. Temperature was kept at 70 °C for 18 h. The pH of the solution was maintained at 9.5 with drops of 5 M NaOH. The solution was then dried under vacuum, the residue dissolved in water (20 mL), and the pH of the solution adjusted to 7 by addition of 5 M HCl. The solution was then passed through a cation-exchange column (Amberlite IR 120; acidic form, bed volume 60 cm^3). The column was eluted with water (500 mL), then with NH_3 0.5 M solution (600 mL), and finally with water (700 mL). Each fraction was vacuum evaporated and analyzed by ^1H NMR. The fractions containing the desired product were pooled together, and the resulting solution was vacuum evaporated, yielding the ligands as ammonium salt. This compound was dissolved in 10 mL of water, and the solution passed through a column filled with an anion-exchange resin (Amberlite IRA 900, alkaline form, bed volume 50 mL). The column was eluted before with water (350 mL), then with a HCl 5 M solution (350 mL), and finally with an HCl 0.1 M solution (300 mL). Each fraction was vacuum evaporated and analyzed by ^1H NMR. The fractions containing the desired product were combined and vacuum evaporated to dryness. The resulting stick oil was suspended in diethyl ether to obtain a white solid, which was filtered off. Yield 1.35 g (50.4%). ^1H NMR (300.07 MHz, D_2O, pH 3.0, 25 °C), δ (ppm): 3.57 (4H, s); 3.49 (4H, dd); 3.31 (4H, dd); δ 3.17 (4H, dd); δ 2.16 ppm (4H, dd). ^{13}C NMR (75 MHz, D_2O, pH 3.0, 25 °C), δ (ppm): 177.0; 54.9; 54.3; 50.1. ESI MS (m/z) 317 ($H_2L4 + H^+$).

Synthesis of [MnL3]. A deoxygenated aqueous solution (10 mL) of $MnSO_4\cdot H_2O$ (170 mg, 1 mmol) was slowly added, under stirring, to a boiling solution of $H_2L3\cdot 2HCl$ (360 mg, 1 mmol) in 30 mL of water under a nitrogen atmosphere. To this solution was slowly added 20 mL of NaOH 0.1 M. The resulting solution was then refluxed for 3 h. The volume of the solvent was then reduced to 5 mL by heating at 80 °C under a nitrogen flow. To the resulting solution, ethanol (30 mL) was added to yield a white precipitate, which was filtered off and recrystallized from an water/ethanol 1:8 mixture. Yield 250 mg (72.3%). ESI MS (m/z): 342 ($[MnL3 + H]^+$).

Synthesis of $[MnL4]\cdot 2H_2O$. A deoxygenated aqueous solution of NaOH 0.1 M (6.9 mL, 0.69 mmol) was added to deoxygenated solution (10 mL) of $H_2L4\cdot 3HCl$ (100 mg, 0.23 mmol) in water. To this solution, heated to reflux, a solution of $MnCl_2\cdot 4H_2O$ (42 mg, 0.21 mmol) was slowly added under stirring in deoxygenated water. The volume of the solvent was then reduced at 5 mL by heating at 80 °C under nitrogen flow. To the resulting solution, ethanol (20 mL) and diethyl ether (10 mL) were added, to yield a white precipitate which was filtered off and recrystallized from a water/ethanol 1:15 mixture. Yield 45 mg (52.9%). ESI MS (m/z): 370 ($[MnL4 + H]^+$).

Potentiometric Measurements. pH-metric measurements ($pH = -\log[H^+]$) were carried out with 0.1 M NMe_4Cl (pK_w = 13.83) at 25.0 ± 0.1 °C, by using the previously described equipment and procedure.[37] The computer program HYPERQUAD[38] was used to calculate both protonation and stability constants from emf data. Distribution diagrams and competition plots were calculate by using the Hyss program.[28] Full experimental details are provided in the Supporting Information.

Microcalorimetric Measurements. The enthalpies of protonation and metal complexation with H_2L3 and H_2L4 were determined in 0.1 M NMe_4Cl aqueous solution 25.0 ± 0.1 °C, by the previously described equipment and procedure.[39] In the protonation and complexation studies, 1×10^{-3} ligand and metal ions concentrations were employed, performing at least three titration experiments. The corresponding enthalpies of reaction were determined from calorimetric data by the AAAL program.[40]

Electrochemical Measurements. Electrochemical characterization was performed using a computerized electrochemical analyzer (CH Instruments Inc., Austin, TX). Electrochemical tests were carried out at room temperature under nitrogen atmosphere, using a conventional single-compartment, three-electrode cell. A Au working electrode (Goodfellow, 3 mm diameter wire, 99.99+% pure) was inserted inside a Teflon tube. The electrode was polished with 1 and 0.3 μm alumina powder and then rinsed with distilled water and sonicated in an ultrasonic bath for 5 min before use. The working electrode potential was measured with respect to an aqueous KCl saturated Ag/AgCl electrode. A platinum wire was used as auxiliary electrode. Measurements were carried out on deareated aqueous solutions at pH 7 containing the Mn(II) complexes at a 5×10^{-4} M concentration. Cyclic voltammograms were recorded on a gold electrode in 0.1 M KNO_3 adjusted to pH 7.0 with 0.1 M NaOH. Superimposition of the oxidation peak of chloride with those of the complexes prevented the use of NaCl as ionic medium. The use of a gold electrode allows better resolution of the oxidation peaks of the complexes.

Scavenging of $O_2^{\bullet-}$ Generated by the Xanthine/Xanthine Oxidase Reaction. *In vitro* generation of $O_2^{\bullet-}$ by the enzymatic reaction of xanthine oxidase (10 mU/mL) with xanthine

(600 μM) was monitored spectrophotometrically at 560 nm measuring the oxidation kinetics of 10 μM nitro blue tetrazolium (NBT) as previously described.[41] Experiments were performed in triplicate. Full experimental details are provided in the Supporting Information.

Scavenging of $O_2^{\bullet-}$ Generated by Activated Macrophages. This experiment aimed at testing the ability of the noted compounds to scavenge $O_2^{\bullet-}$ in a cellular system. RAW 264.7 cells were grown until confluent (5×10^3) in 96-well plates, starved for 18 h, and incubated in phenol red-free DMEM containing 1 mg/mL cytochrome C, in the presence or absence of the Mn(II) complexes at different concentrations. Cells were stimulated with 0.1 μM N-formyl-Met-Leu-Phe peptide (fMLP) for 4 h at 37 °C. The cytochrome C reduced form was measured spectrophotometrically at 550 nm. Blank tests were carried out in the presence of 300 U/mL MnSOD, and these absorbance values were subtracted to their respective values. The Mn(II) complexes did not interfere with cytochrome C absorbance. In parallel experiments, RAW264.7 cells were preincubated for 18 h with [MnL4] (0.1 μM), washed twice, and stimulated with 0.1 μM fMLP in the presence or absence of 0.1 μM [MnL4] for 4 h at 37 °C as described above. The SOD-inhibitable $O_2^{\bullet-}$ production was expressed as μmol/mL/10^6 cells using an extinction coefficient of 2.1×10^4 M/cm. Experiments were performed in quadruplicate on at least 3 different cell batches. Full experimental details are given in the Supporting Information.

Isolation and Culture of Rat Aorta Smooth Muscle Cells (RASM). Smooth muscle cells were isolated from rat thoracic aortas by enzymatic digestion as described[42] and used between the fifth and ninth passage in culture.

Mn(II) Complexes Bioavailability in Cell Culture. To evaluate the cellular bioavailability of Mn(II) compounds, confluent RASM cells were incubated for 6 h in PBS (containing $CaCl_2$ and $MgCl_2$) in control conditions or in the presence of $MnSO_4$ or the Mn(II) complexes (10 μM). Cells were then washed twice, lysed in bidistilled H_2O, frozen, and kept at −80 °C until use. Aliquots were used for total protein dosage. Determination of total manganese content in the cell lysates was performed by a Varian 720-ES ICP-AES. Before analysis, about 3 mg of sample was weighed in polyethylene tubes and solubilized in 10 mL of 0.1% suprapure nitric acid obtained by sub-boiling distillation. To promote solubilization and homogenization of the solutions, the tubes were placed into an ultrasonic bath for 15 min. Samples were spiked with 1 ppm of Ge used as internal standard and calibration standards were prepared by gravimetric serial dilution from mono standards at 1000 mg/L. Wavelengths used for ICP-AES analysis and operating conditions, optimized to obtain a maximum signal intensity, instrumental conditions, and measurement, are reported in the Supporting Information. Within each sample, a rinsing solution composed by 2% v/v HNO_3 was used. The ICP torch, spray chamber, nebulizer, and sample introduction tubes were accurately cleaned and, prior to sample analysis, the instrument was purged for at least 1 h with 2% v/v HNO_3 rinse solution. Experiments were performed on 3 different cell batches.

Cell Viability Assay. Cell viability was evaluated by the reduction of 3-(4,5-dimethylthiozol-2-yl)-2,5-diphenyltetrazolium bromide (MTT). RAW264.7 cells were grown until confluence (5×10^3) into 96 well plates cells, starved for 12 h, and then treated for 24, 48, and 72 h with different concentrations of [MnL4]·$2H_2O$ (0.1−100 μM) in 0.1% FBS medium. After extensive washing, 1 mg/mL MTT was added into each well and incubated for 2 h at 37 °C. After washing, the formazan crystals were dissolved in 100 μL dimethyl sulfoxide. The absorbance was measured at 580 nm. Experiments were performed in quadruplicate on at least 3 different cell batches .

Inhibition of ROS-Induced Cell Oxidative Injury. Cell membrane lipid peroxidation was evaluated as thiobarbituric acid reagent substances (TBARS)[31] in RASM cells ($1.2-1.5 \times 10^6$). To induce lipid peroxidation, two different sources of $O_2^{\bullet-}$ were used: xanthine/xanthine oxidase or fMLP-activated RAW264.7 macrophages. RASM cells were treated for 4 h at 37 °C either with 600 μM xanthine/xanthine oxidase (10 mU/mL) or with unstimulated or 0.1 μM fMLP-stimulated RAW264.7 ($1-1.2 \times 10^5$, grown on trans-well inserts, 0.4 μm pore size) . Both protocols were performed in the absence or presence of either 0.1 μM [MnL4]·$2H_2O$ or 300 U/mL MnSOD. Lipid peroxidation was also evaluated in RASM cells treated for 4 h at 37 °C with 20 μM $FeCl_3$/100 μM ascorbic acid, a chemical source of hydroxyl radical.[43] After incubations, RASM cells were placed in ice-cold bath, harvested, and centrifuged. After homogenization in 100 mM potassium phosphate buffer (pH7.4), aliquots of homogenates were used to measure TBARS.[31] TBARS were expressed as nmol/mg protein/mL by comparison with a standard curve of 1,1,3,3-tetramethoxypropane. Experiments were performed on 3 different cell batches. Full experimental details are provided in the Supporting Information.

***In Vivo* Experiments.** Animal handling was carried out according to the European Community guidelines for animal care (DL 116/92, application of the European Communities Council Directive 86/609/EEC). The ethical policy of the University of Florence conforms with the Guide for the Care and Use of Laboratory Animals of the U.S. National Institutes of Health (NIH Publication No. 85−23, revised 1996; University of Florence assurance number: A5278−01). Formal approval to conduct the experiments described herein was obtained from the animal subjects review board of the University of Florence. For the experiments described, male albino CD1 mice, 20−25 g, were used. They were purchased from Harlan Italy (Udine, Italy) and quarantined for 1 week before use.

Toxicity Assay. Animals were randomly assigned to 3 different groups (each group, $n = 5$). [MnL4]·$2H_2O$ was dissolved in saline and administered intraperitoneally (i.p.) at 100 and 200 mg/kg body weight (b.wt) and its effects observed for 4 h after injection. The negative controls ($n = 5$) received the vehicle alone. The animals were monitored daily for up to 1 week.

Anti-Inflammatory and Analgesic Assay. The putative anti-inflammatory properties of [MnL4]·$2H_2O$ were investigated in the mouse writhing test.[44] Mice, randomly distributed in different groups, were injected i.p. with 0.6% acetic acid and, 5 min later, the number of writhes due to abdominal constriction was counted for further 10 min. [MnL4]·$2H_2O$ or H_2L4 at the doses of 1, 5, and 15 mg/kg b.wt, indomethacin (10 mg/kg b.wt), or the vehicle (1% carboxymethylcellulose) were administered by a gastric catheter (p.os) 15−30 min before acetic acid injection. In parallel experiments, [MnL4] or H_2L4, dissolved in saline at the same doses, were administered i.p. 15 min before acetic acid injection. Morphine-like analgesic activities of compounds were determined on a hot-plate test.[45] [MnL4] or H_2L4, dissolved in saline at the same doses, were administered i.p. 15 min before testing mice reaction time (s) on a hot plate (52.5 °C). Morphine (10 mg/kg b.wt) was used as reference drug.

Statistical Analysis. Data are reported as means ± standard errors of means (S.E.M.) and were analyzed for statistical comparison by one-way ANOVA followed by Bonferroni's *posthoc* test. Differences were considered significant if $p < 0.05$.

Acknowledgment. This work was supported by funds from the University of Florence, Italy.

Supporting Information Available: Experimental details for potentiometric measurements and for experiments on $O_2^{\bullet-}$ scavenging and on inhibition of ROS-induced cell oxidative injury, elemental analysis for tested compounds, thermodynamic parameters for protonation of H_3L1, H_4L2, H_2L3, and H_2L4, operating conditions for ICP-AES measurements, distribution diagrams for the Mn(II) complexes with H_3L1 and H_4L2, competition plots for H_4L2 and H_2L3 in the presence of Mn(II) (1 μM), Ca(II), (2.5 mM), Mg(II) (1.2 mM), and Na(I)

(165 mM), competition plots for H_3L1, H_4L2, H_2L3, and H_2L4 in the presence of Mn(II) (1 μM), Ca(II), (10 mM), Mg(II) (10 mM), and Na(I) (200 mM). This material is available free of charge via the Internet at http://pubs.acs.org.

References

(1) Fridovich, I. Superoxide Dismutases. An Adaptation to a Paramagnetic Gas. *J. Biol. Chem.* **1989**, *264*, 7761–7764.
(2) Johnson, F.; Giulivi, C. Superoxide Dismutases and their Impact upon Human Health. *Mol. Aspects Med.* **2005**, *26*, 340–352.
(3) Finkel, T. Radical Medicine: Treating Ageing to Cure Disease. *Nat. Rev. Mol. Cell. Biol.* **2005**, *6*, 971–976.
(4) Wang, Z. Q.; Porreca, F.; Cuzzocrea, S.; Galen, K.; Lightfoot, R.; Masini, E.; Muscoli, C.; Mollace, V.; Ndengele, M.; Ischiropoulos, H.; Salvemini, D. A Newly Identified Role for Superoxide in Inflammatory Pain. *J. Pharmacol. Exp. Ther.* **2004**, *309*, 869–878.
(5) Petkau, A. Scientific Basis for the Clinical Use of Superoxide Dismutase. *Cancer Treat. Rev.* **1986**, *13*, 17–44.
(6) McCord, J. M.; Edeas, M. A. SOD, Oxidative Stress and Human Pathologies: a Brief History and a Future Vision. *Biomed. Pharmacother.* **2005**, *59*, 139–142.
(7) Slemmer, J. E.; Shacka, J. J.; Sweeney, M. I.; Weber, J. T. Antioxidants and Free Radical Scavengers for the Treatment of Stroke, Traumatic Brain Injury and Aging. *Curr. Med. Chem.* **2008**, *15*, 404–414.
(8) Riley, D. P.; Weiss, R. H. Manganese Macrocyclic Ligand Complexes as Mimics of Superoxide Dismutase. *J. Am. Chem. Soc.* **1994**, *116*, 387–388.
(9) Sheng, H.; Enghild, J. J.; Bowler, R.; Pate, M.; Batinic-Haberle, I.; Calvi, C. L.; Day, B. J.; Pearlstein, R. D.; Crapo, J. D.; Warner, D. S. Effect of Metalloporphyrin Catalytic Antioxidants in Experimental Brain Ischemia. *Free Radic. Biol. Med.* **2002**, *33*, 947–961.
(10) Baker, K.; Bucay Marcus, C.; Kruk, H.; Malfroy, B.; Doctrow, S. R. Synthetic Combined Superoxide Dismutase/Catalase Mimetics are Protective as a Delayed Treatment in a Rat Stoke Model: a Key Role for a Reactive Oxygen Species in Ischemic Brain Injury. *J. Pharmacol. Exp. Ther.* **1998**, *284*, 215–221.
(11) Muscoli, C.; Cuzzocrea, S.; Riley, D. P.; Zweier, J. L.; Thiemermann, C.; Wang, Z.-Q.; Salvemini, D. On the Selectivity of a Superoxide Dismutase Mimetics and its Importance in Pharmacological Studies. *Br. J. Pharmacol.* **2003**, *140*, 445–460.
(12) Salvemini, D.; Riley, D. P.; Cuzzocrea, S. Sod Mimetics are Coming of Age. *Nat. Rev.* **2002**, 367–374.
(13) Salvemini, D.; Wang, Z. Q.; Zweier, J. L.; Samouilov, A.; Macarthur, H.; Misko, T. P.; Currie, M. G.; Cuzzocrea, S.; Sikorski, J. A.; Riley, D. P. A Non-Peptidyl Mimic of Superoxide Dismutase with Therapeutic Activity in Rats. *Science* **1999**, *286*, 304–306.
(14) Masini, E.; Cuzzocrea, S.; Mazzon, E.; Marzocca, C.; Mannaioni, P. F.; Salvemini, D. Protective Effects of M40403, a Selective Superoxide Dismutase Mimetic, in Myocardial Ischaemia and Reperfusion Injury in Vivo. *Br. J. Pharmacol.* **2002**, *136*, 905–917.
(15) Masini, E.; Bani, D.; Vannacci, A.; Pierpaoli, S.; Mannaioni, P. F.; Comhair, S. A.; Xu, W.; Muscoli, C.; Erzurum, S. C.; Salvemini, D. Reduction of Antigen-Iinduced Respiratory Abnormalities and Airway Inflammation in Sensitized Guinea Pigs by a Superoxide Dismutase Mimetic. *Free Radic. Biol. Med.* **2005**, *39*, 520–531.
(16) Cotton, F. A.; Wilkinson, G. *Advanced Inorganic Chemistry*; John Wiley & Sons: New York, 1988.
(17) Fricker, S. P. Metal Complexes as Therapeutic Agents in Nitrogen Monoxide Modulation. In *Metal Ions in Biological Systems*, Vol 41: Metal Ions and their Complexes in Medication, Sigel, A., Sigel, H., Eds.; Marcel Dekker: New York, 2004, pp 421−480.
(18) Edwards, H. *Powdered Detergents*, Showell, M. S., Ed.; Marcel Dekker: New York,1988.
(19) Elihu, N.; Anandasbapathy, S.; Frishman, W. H. Chelation Therapy in Cardiovascular Disease: Ethylenediaminetetraacetic Acid, Deferoxamine, and Dexrazoxane. *J. Clin. Pharmacol.* **1998**, *38*, 101–105.
(20) Merbach, A. E.; Tóth, E. *The Chemistry of Contrast Agents in Medical Magnetic Resonance Imaging*; John Wiley & Sons: New York, 2001.
(21) Bianchi, A.; Calabi, L.; Corana, F.; Fontana, S.; Losi, P.; Maiocchi, A.; Paleari, L.; Valtancoli, B. Thermodynamics and Structural Properties of Gd(III) Complexes with Polyamino-Polycarboxylic Ligands: Basic Compound for the Development of MRI Contrast Agents. *Coord. Chem. Rev.* **2000**, *24*, 309–393.
(22) McCleverty, J. A. Chemistry of Nitric Oxide Relevant to Biology. *Chem. Rev.* **2004**, *104*, 403–418.
(23) Bambagioni, V.; Bani, D.; Bencini, A.; Biver, T.; Cantore, M.; Chelli, R.; Cinci, M.; Failli, P.; Ghezzi, L.; Giorgi, C.; Nappini, S.; Secco, F.; Tinè, M. R.; Valtancoli, B.; Venturini, M. Polyamine-Polycarboxylate Metal Complexes with Different Biological Effectiveness as Nitric Oxide Scavengers. Clues for Drug Design. *J. Med. Chem.* **2008**, *51*, 3250–3260.
(24) Schmidt, C. K; Brauch, H.-J. Impact of Aminopolycarboxylates on Aquatic Organisms and Eutrophication: Overview of Available Data. *Environ. Toxicol.* **2004**, *19*, 620–37.
(25) Bencini, A.; Bianchi, A.; Garcia-España, E.; Micheloni, M.; Ramirez, J. A. Proton Coordination by Polyamine Compounds in Aqueous Solution. *Coord. Chem. Rev.* **1999**, *188*, 97–156.
(26) Mathur, R. P.; Mathur, P. N. Composition and Stability Constants of N-(2-hydroxyethyl)ethylenediamine-N,N′,N′-Ttriacetic Acid Complexes of Barium(II), Strontium(II), Calcium(II), and Magnesium(II). *Indian J. Chem.* **1981**, *20A*, 309–311.
(27) Smith, G. L.; Miller, D. J. Potentiometric Measurements of Stoichiometric and Apparent Affinity Constants of EGTA for Protons and Divalent Ions Including Calcium. *Biochim. Biophys. Acta* **1985**, *839*, 287–299.
(28) Alderighi, L.; Gans, P.; Ienco, A.; Peters, D.; Sabatini, A.; Vacca, A. Hyperquad Simulation and Speciation (HySS): A Utility Program for the Investigation of Equilibria Involving Soluble and Partially Soluble Species. *Coord. Chem. Rev.* **1999**, *184*, 311–318.
(29) Bianchi, A.; Garcia-España, E. The Use of Calculated Species Distribution Diagrams to Analyze Thermodynamic Selectivity. *J. Chem. Educ.* **1999**, *76*, 1727–1732.
(30) Bockris, J. O. M.; Reddy, A. K. N.; Aldeco M. G. *Modern Electrochemistry*; Kluver Academic Plenum Publishers: New York, 2000.
(31) Rao, P. S.; Cohen, M. V.; Mueller, H. S. Production of Free Radicals and Lipid Peroxides in Early Experimental Myocardial Ischemia. *J. Mol. Cell. Cardiol.* **1983**, *15*, 713–716.
(32) The proposed structure in Scheme 3 was sketched considering that bivalent first-row transition metal cations, including Mn(II), are generally too large to fit inside the small macrocyclic cavity of 1,4,7,10-tetraazacyclododecane or its derivatives and therefore the metals lie upon the mean plane (in some cases even more than 1 Å), determined by the four amine donors. In 6-coordinate metal complexes, the additional donor atoms generally prefer to assume a cis disposition. Closest comparisons with the present case can be found in the recent crystal structure obtained for the Mn(II) complex with compound 1,4,7,10-tetraazacyclododecane-1,4,7,10-tetraacetic acid, which contains the same tetraamine units of H2L3 (see Wan, S.; Westmoreland, T. D. Correlation of Relaxivity with Coordination Number in Six-, Seven-, and Eight-Coordinate Mn(II) Complexes of Pendant-Arm Cyclen Derivatives. *Inorg. Chem.* **2009**, *48*, 719−727). In fact, in this complex the metal cation is bound by the four amine groups and two deprotonated carboxylate groups in 1,7 position (the remaining two carboxylic groups are not involved in metal binding); the two coordinated carboxylate groups assume a cis disposition within the overall coordination sphere, in a similar fashion to that sketched in Scheme 3 for [MnL3] and [MnL4].
(33) Bencini, A.; Bianchi, A.; Micheloni, M.; Paoletti, P.; Garcia-España, E.; Niño, M. A. Co-ordination Tendency of [3k]aneN$_k$ Polyazacycloalkanes. Thermodynamic Study of Solution Equilibria. *J. Chem. Soc., Dalton Trans.* **1991**, 1171–1174.
(34) Meyerstein, D.; Are, M-N Bonds Indeed Inherently Weaker when N is a Tertiary Rather than a Primary or Secondary Nitrogen Atom? *Coord. Chem. Rev.* **1999**, *186*, 141–147.
(35) Kovacs, Z.; Sherry, A. D. A General Synthesis of 1,7-Disubstituted 1,4,7,10-Tetraazacyclododecanes. *J. Chem. Soc., Chem. Commun.* **1995**, 185–186.
(36) Barbaro, P.; Bianchini, C.; Capannesi, G.; Di Luca, L.; Laschi, F.; Petroni, D.; Salvadori, P. A.; Vacca, A.; Vizza, F. Synthesis and Characterization of the Tetraazamacrocycle 4,10-Dimethyl-1,4,7,10-Tetraazacyclododecane-1,7-Diacetic Acid (H_2Me_2-DO2A) and its Neutral Complex [Cu(Me_2DO2A)]. A New ^{64}Cu-Labeled Macrocyclic Complex for Positron Emission Tomography Imaging. *J. Chem. Soc., Dalton Trans.* **2000**, 2393–2401.
(37) Lodeiro, C.; Parola, A. J.; Pina, F.; Bazzicalupi, C.; Bencini, A.; Bianchi, A.; Giorgi, C.; Masotti, A.; Valtancoli, B. Protonation and Zn(II) Coordination by Dipyridine-containing Macrocycles with Different Molecular Architecture. A Case of pH-controlled Metal Jumping Outside-inside the Macrocyclic Cavity. *Inorg. Chem.* **2001**, *40*, 2968–2975.
(38) Gans, P.; Sabatini, A.; Vacca, A. Investigation of Equilibria in Solution. Determination of Equilibrium Constants with HYPERQUAD Suite of Programs. *Talanta* **1996**, *43*, 1739–1753.
(39) Bazzicalupi, C.; Bencini, A.; Fusi, V.; Giorgi, G.; Paoletti, P.; Valtancoli, B. Lead Complexation by Novel Phenanthroline-Containing Macrocycles. *J. Chem. Soc., Dalton Trans.* **1999**, 393–400.
(40) Vacca, A. *AALL program*; University of Florence, **1997**.

(41) Ciuffi, M.; Cellai, C.; Franchi-Micheli, S.; Failli, P.; Zilletti, L.; Ginanneschi, M.; Chelli, M.; Papini, A. M.; Paletti, F. An in Vivo, ex Vivo and in Vitro Comparative Study of Activity of Copper Oligopeptide Complexes vs Cu(II) Ions. *Pharmacol. Res.* **1998**, *38*, 279–287.
(42) Mazzetti, L.; Franchi-Micheli, S.; Nistri, S.; Quattrone, S.; Simone, R.; Ciuffi, M.; Zilletti, L.; Failli, P. The ACh-Induced Contraction in Rat Aortas is Mediated by the Cys Lt_1 Receptor Via Intracellular Calcium Mobilisation in Smooth Muscle Cells. *Br. J. Pharmacol.* **2003**, *138*, 707–715.
(43) Cohen G. The Fenton Reaction. In *Handbook of Methods for Oxygen Radical Research*., Greenwald, R. A., Ed.; CRC Press: Boca Raton, FL, 1986; pp 55−64.
(44) Koster, R.; Anderson, M.; de Beer, E. J. Acetic Acid for Analgesic Screening. *Fed. Proc.* **1959**, *18*, 412–418.
(45) Galeotti, N.; Quattrone, A.; Vivoli, E.; Bartolini, A.; Ghelardini, C. Knockdown of the Type 2 and 3 Inositol 1,4,5-Trisphosphate Receptors Suppresses Muscarinic Antinociception in Mice. *Neuroscience* **2007**, *149*, 409–420.